ELSEVIER

Catalysis Today 54 (1999) 391–400

CATALYSIS TODAY

www.elsevier.com/locate/cattod

Enhanced activity of metal oxide-doped Ga_2O_3–Al_2O_3 for NO reduction by propene

Masaaki Haneda *, Yoshiaki Kintaichi, Hideaki Hamada

National Institute of Materials and Chemical Research, 1-1 Higashi, Tsukuba, Ibaraki 305-8565, Japan

Abstract

Effect of additives, In_2O_3, SnO_2, CoO, CuO and Ag, on the catalytic performance of Ga_2O_3–Al_2O_3 prepared by sol–gel method for the selective reduction of NO with propene in the presence of oxygen was studied. As for the reaction in the absence of H_2O, CoO, CuO and Ag showed good additive effect. When H_2O was added to the reaction gas, the activity of CoO-, CuO- and Ag-doped Ga_2O_3–Al_2O_3 was depressed considerably, while an intensifying effect of H_2O was observed for In_2O_3- and SnO_2-doped Ga_2O_3–Al_2O_3. Of several metal oxide additives, In_2O_3-doped Ga_2O_3–Al_2O_3 showed the highest activity for NO reduction by propene in the presence of H_2O. Kinetic studies on NO reduction over In_2O_3–Ga_2O_3–Al_2O_3 revealed that the rate-determining step in the absence of H_2O is the reaction of NO_2 formed on Ga_2O_3–Al_2O_3 with C_3H_6-derived species, whereas that in the presence of H_2O is the formation of C_3H_6-derived species. We presumed the reason for the promotional effect of H_2O as follows: the rate for the formation of C_3H_6-derived species in the presence of H_2O is sufficiently fast compared with that for the reaction of NO_2 with C_3H_6-derived species in the absence of H_2O. Although the retarding effect of SO_2 on the activity was observed for all of the catalysts, SnO_2–Ga_2O_3–Al_2O_3 showed still relatively high activity in the lower temperature region. ©1999 Elsevier Science B.V. All rights reserved.

Keywords: Nitrogen monoxide; Selective reduction; H_2O; In_2O_3–Ga_2O_3–Al_2O_3; SnO_2–Ga_2O_3–Al_2O_3; Sol–gel method; Kinetic studies; SO_2

1. Introduction

The selective catalytic reduction of NO with hydrocarbons in the presence of oxygen has been studied extensively as a practical measure to remove NO_x in diesel and lean burn engine exhausts [1,2]. A lot of effective catalysts, such as metal ion-exchanged zeolites [3–6], noble metals [7–9], alumina [10] and transition metal supported alumina [11–13], have been reported so far. Exhaust gases usually contain H_2O and SO_2 affecting the catalytic performance. Although zeolite-based catalysts show high catalytic activity at high space velocities, their deactivation under hydrothermal conditions due to dealumination from the framework is a serious problem from a practical viewpoint [14–16]. On the other hand, alumina-based catalysts are attracting attention because of their high stability. However, coexisting H_2O and SO_2 often inhibit the selective reduction of NO over alumina-based catalysts. Hence, development of novel catalysts showing high activity and durability in the presence of H_2O and SO_2 is required.

Recently, we reported that Ga_2O_3–Al_2O_3 catalyst prepared by sol–gel method showed quite high activity for NO reduction by propene in the presence of oxygen, H_2O and SO_2 [17]. However, the effective temperature window for NO reduction was relatively narrow and was located in the high temperature region. In the present study, we investigated the

* Corresponding author. Fax: +81-298-54-4487
E-mail address: hane@nimc.go.jp (M. Haneda)

0920-5861/99/$ – see front matter ©1999 Elsevier Science B.V. All rights reserved.
PII: S0920-5861(99)00202-3

effect of metal oxide additives on Ga_2O_3–Al_2O_3 for the selective reduction of NO with propene, in order to promote the NO reduction activity in the presence of H_2O and SO_2 at low temperatures. In the course of our study, we found that coexisting H_2O promoted considerably NO reduction over some catalysts, especially In_2O_3-doped Ga_2O_3–Al_2O_3. Therefore, we made some kinetic studies on this catalyst. We also studied the influence of coexisting SO_2 on the activity of the metal oxide-doped catalysts.

2. Experimental

2.1. Catalysts

Metal oxide-doped Ga_2O_3–Al_2O_3 catalysts were prepared by coprecipitation through sol–gel process. In, Sn, Co, Cu and Ag were selected as the additives. Aluminium boehmite sol was first prepared by hydrolysis of aluminium(III) tri-isopropoxide in hot water (363 K) with a small amount of nitric acid, and then mixed with a solution of gallium(III) nitrate and metal nitrate of the doped metal oxide, except for Sn for which tin chloride was used, in ethylene glycol. After the sol solution was stirred for 1 day, the solvents were eliminated by heating under reduced pressure. All the catalyst precursors were dried at 383 K, followed by calcination at 873 K for 5 h in flowing air. Some catalyst samples were further calcined at 1073 K for 5 h in air. The loading of metal oxide and Ga_2O_3 was fixed at 5 and 30 wt.%, respectively. In the case of Ag, the loading was calculated as Ag-metal. Al_2O_3 and Ga_2O_3–Al_2O_3 with Ga_2O_3 loading of 30 wt.% were also prepared as reference samples by the same sol–gel method. The resulting powders were calcined finally at 873 K for 5 h in flowing air.

2.2. Catalytic reaction

2.2.1. Activity measurements

The catalytic activity was measured by using a fixed-bed flow reactor. 0.2 g of a catalyst sample was used, unless otherwise specified. The feed gas mixture contained 900 ppm NO, 900 ppm C_3H_6 as a reducing agent, 10% oxygen and helium as the balance gas. The gas flow rate was fixed at 66 $cm^3\,min^{-1}$ (W/F = 0.18 $gscm^{-3}$, SV = 10 000 h^{-1}). In some experiments, H_2O and SO_2 were introduced into the reaction gas mixture at a concentration of 9.1% and 90 ppm, respectively. H_2O was introduced with micropump. Prior to the activity measurement in the presence of SO_2, the catalyst was treated at 773 K for 12 h in a flowing gas containing 900 ppm NO, 10% O_2, 300 ppm SO_2 and 9.1% H_2O diluted in He with a gas flow rate of 66 $cm^3\,min^{-1}$, in order to stabilize the catalyst. In these cases, the feed gas flow rate and the concentrations of the other gas components were not changed by controlling the helium flow rate. The reaction temperature was changed from 873 to 523 K with a step of 50 K. The effluent gas was analyzed by gas chromatography.

A molecular-sieve 5A column was used for the analysis of N_2 and CO and a Porapak Q column for that of N_2O, CO_2 and C_3H_6. The catalytic activity was evaluated in terms of NO conversion to N_2 and that of propene to CO_x ($CO + CO_2$). The formation of N_2O was found negligible in the present study.

2.2.2. Kinetic studies

For In_2O_3–Ga_2O_3–Al_2O_3, the reaction rate of N_2 formation was evaluated by changing the catalyst weight from 0.03 to 0.1 g to obtain a conversion level of NO in the range of 10–30%. The kinetic parameters for N_2 and CO_x formation were determined at 623 K in the presence and absence of H_2O by changing the concentrations of the reactants in the range of 200–1500 ppm for NO, 200–1500 ppm for C_3H_6 and 3–10% for O_2. The total flow rate was 66 $cm^3\,min^{-1}$. The standard reaction conditions were 900 ppm NO, 900 ppm C_3H_6, 10% oxygen and 0 or 9.1% H_2O. The activation energy was calculated at temperatures ranging from 623 to 723 K under the standard reaction conditions.

2.3. Catalyst characterization

BET surface area was measured by nitrogen adsorption at 77 K with a conventional flow type apparatus (Micromeritics, Flowsorb II 2300). The crystallite structure was identified by XRD measurements (Shimadzu XD-D1) by using Cu Kα radiation at 40 kV and 40 mA.

Temperature programmed desorption (TPD) experiments of NO_x were carried out by using 50 mg of a sample. The sample was pretreated in a flow of 10% O_2/He at 873 K for 1 h and then cooled to room temperature. NO_x adsorption was performed by passing a gas mixture containing 1000 ppm NO and 10% O_2 diluted in He through the sample bed at room temperature for 2 h. After the adsorption gas was purged with He until no NO was detected in the effluent, the TPD measurement was carried out up to 873 K with a heating rate of 5 K min^{-1} in flowing He. The gas flow rate was fixed at 60 cm^3 min^{-1}. The desorbed species with a mass number of 30 (NO), 32 (O_2) and 46 (NO_2) were monitored continuously by a quadruple mass spectrometer (ANELVA M-QA200TS) as a function of temperature.

3. Results and discussion

3.1. Additive effect of metal oxides

Fig. 1 shows the activity of In_2O_3-, SnO_2-, CoO-, CuO- and Ag-doped Ga_2O_3–Al_2O_3 calcined at 873 K for NO reduction by propene in the absence of H_2O. Although Ga_2O_3–Al_2O_3 catalyzed effectively the NO reduction by propene with high NO conversion more than 90% in the temperature range of 673–823 K, the addition of CoO, CuO and Ag enhanced further the activity of Ga_2O_3–Al_2O_3 in the lower temperature region below 623 K. The maximum NO conversion on CuO- and Ag–Ga_2O_3–Al_2O_3, however, was much less than that on Ga_2O_3–Al_2O_3. This is because propene oxidation by oxygen, which is a side reaction consuming propene, proceeds predominantly because of the too high oxidation activity of CuO and Ag. In the case of In_2O_3 and SnO_2, NO reduction was also decreased, although their propene oxidation activity was not so high.

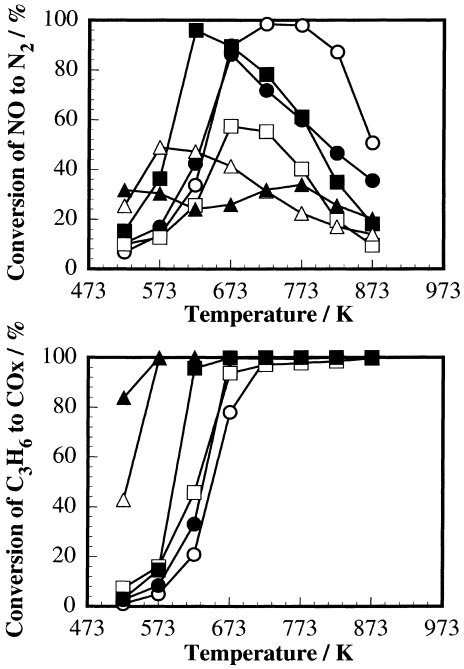

Fig. 1. Additive effect of metal oxides on the catalytic activity of Ga_2O_3–Al_2O_3 calcined at 873 K for NO reduction by propene in the absence of H_2O. Conditions: NO = 900 ppm, C_3H_6 = 900 ppm, O_2 = 10%, H_2O = 0%, catalyst weight = 0.2 g, W/F = 0.18 g s cm^{-3}. (○) Ga_2O_3–Al_2O_3, (●) In_2O_3–Ga_2O_3–Al_2O_3, (□) SnO_2–Ga_2O_3–Al_2O_3, (■) CoO–Ga_2O_3–Al_2O_3, (△) CuO–Ga_2O_3–Al_2O_3, (▲) Ag–Ga_2O_3–Al_2O_3.

Table 1
BET surface area of metal oxide-doped Ga_2O_3–Al_2O_3 calcined at 873 or 1073 K

Catalyst	BET surface area (m^{-2} g^{-1})	
	Calcination temperature (K)	
	873	1073
Ga_2O_3–Al_2O_3	200	125
In_2O_3–Ga_2O_3–Al_2O_3	185	135
SnO_2–Ga_2O_3–Al_2O_3	200	140
CoO–Ga_2O_3–Al_2O_3	175	125
CuO–Ga_2O_3–Al_2O_3	175	120
Ag–Ga_2O_3–Al_2O_3	180	135

3.2. Characterization of catalysts

As summarized in Table 1, no great difference in BET surface area was observed among the catalysts prepared here. Fig. 2 shows the XRD patterns of In_2O_3-, SnO_2-, CoO-, CuO- and Ag-doped Ga_2O_3–Al_2O_3 calcined at 873 K along with non-doped Ga_2O_3–Al_2O_3. For all the catalysts, the diffraction peaks assigned to γ-Al_2O_3 and $GaAlO_3$ were detected. As for the catalysts containing In_2O_3, SnO_2 and CoO, no peaks ascribed to each metal oxide additive were observed, meaning the presence of highly dispersed metal oxides. On the other hand, as

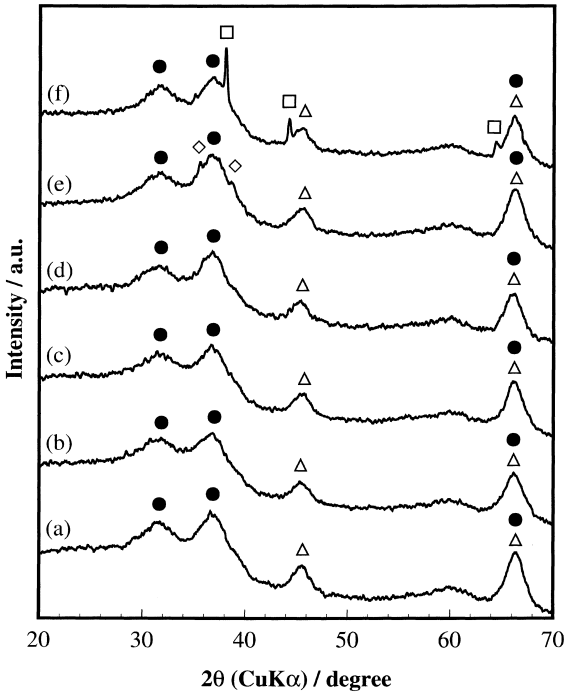

Fig. 2. XRD patterns of (a) Ga_2O_3–Al_2O_3, (b) In_2O_3–Ga_2O_3–Al_2O_3, (c) SnO_2–Ga_2O_3–Al_2O_3, (d) CoO–Ga_2O_3–Al_2O_3, (e) CuO–Ga_2O_3–Al_2O_3 and (f) Ag–Ga_2O_3–Al_2O_3 calcined at 873 K. (△) for γ-Al_2O_3, (●) for $GaAlO_3$, (◇) for CuO, (□) for Ag.

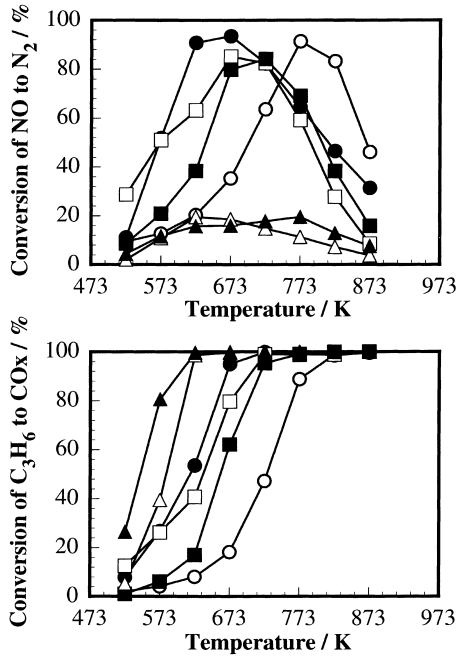

Fig. 3. Effect of H_2O on the catalytic activity of metal oxide-doped Ga_2O_3–Al_2O_3 calcined at 873 K for NO reduction by propene. Conditions: NO = 900 ppm, C_3H_6 = 900 ppm, O_2 = 10%, H_2O = 9.1%, catalyst weight = 0.2 g, W/F = 0.18 gscm^{-3}.(○) Ga_2O_3–Al_2O_3, (●) In_2O_3–Ga_2O_3–Al_2O_3, (□) SnO_2–Ga_2O_3–Al_2O_3, (■) CoO–Ga_2O_3–Al_2O_3, (△) CuO–Ga_2O_3–Al_2O_3, (▲) Ag–Ga_2O_3–Al_2O_3.

can be seen in Fig. 2, CuO- and Ag–Ga_2O_3–Al_2O_3 gave the diffraction peaks assigned to CuO and Ag, respectively, indicating the presence of large CuO and Ag crystals. It has been reported that highly dispersed Cu such as in the form of a spinel phase like $CuAl_2O_4$ [18] and partially oxidized Ag [19–21] are active for the present reaction. Therefore, the presence of large CuO and Ag particles is one of the reasons for their low NO reduction and high propene oxidation activity.

3.3. Effect of H_2O

Fig. 3 shows the activity of the metal oxide-doped Ga_2O_3–Al_2O_3 for NO reduction by propene in the presence of H_2O. As can be seen by comparing Figs. 1 and 3, the activity of Ga_2O_3–Al_2O_3 was depressed considerably by coexisting H_2O and the temperature window became narrow and shifted to higher temperature region. A similar retarding effect of H_2O was observed for CoO-, CuO- and Ag–Ga_2O_3–Al_2O_3. On the other hand, a considerable promotional effect was observed for In_2O_3- and SnO_2–Ga_2O_3–Al_2O_3, especially in the lower temperature region below 623 K. NO conversion at 623 K on the former catalyst was increased considerably from 42 to 91% and that on the latter one was increased from 26 to 63%.

3.4. Influence of high-temperature calcination

It is known that calcination temperature is one of the factors affecting the catalytic performance [22–25]. For example, the activity of Co/Al_2O_3 with high cobalt loading was reported to increase with increasing calcination temperature up to 1073 K [22]. Accordingly, we examined the effect of calcination temperature on the activity of metal oxide-doped Ga_2O_3–Al_2O_3 for NO reduction by propene in the presence of H_2O. The activities of the catalysts calcined at 1073 K are shown in Fig. 4. As can be seen by comparing Figs. 3 and 4, NO conversion as well as propene conversion on all the catalysts was hardly affected by calcination at

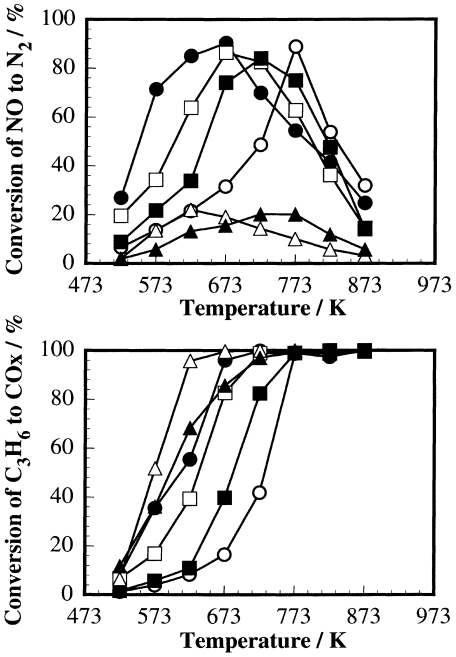

Fig. 4. Catalytic activity of metal oxide-doped Ga_2O_3–Al_2O_3 calcined at 1073 K for NO reduction by propene in the presence of H_2O. The reaction conditions are the same as for Fig. 3. (○) Ga_2O_3–Al_2O_3, (●) In_2O_3–Ga_2O_3–Al_2O_3, (□) SnO_2–Ga_2O_3–Al_2O_3, (■) CoO–Ga_2O_3–Al_2O_3, (△) CuO–Ga_2O_3–Al_2O_3, (▲) Ag–Ga_2O_3–Al_2O_3.

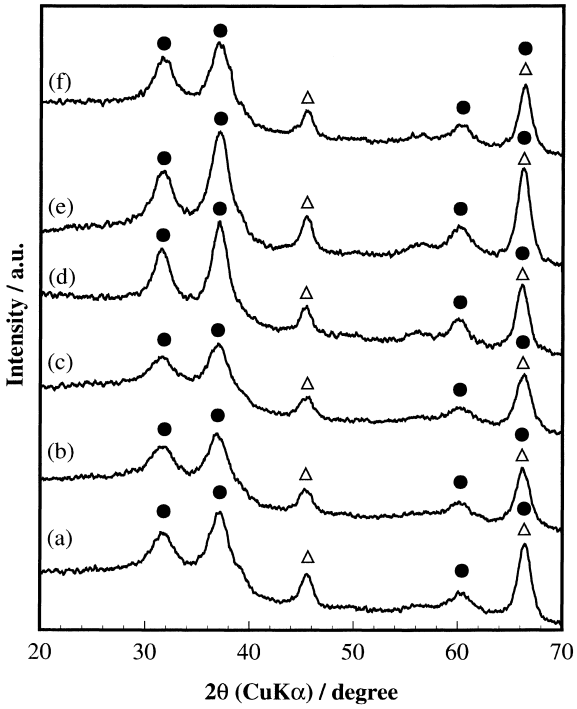

Fig. 5. XRD patterns of (a) Ga_2O_3–Al_2O_3, (b) In_2O_3–Ga_2O_3–Al_2O_3, (c) SnO_2–Ga_2O_3–Al_2O_3, (d) CoO–Ga_2O_3–Al_2O_3, (e) CuO–Ga_2O_3–Al_2O_3 and (f) Ag–Ga_2O_3–Al_2O_3 calcined at 1073 K. (△) for γ-Al_2O_3, (●) for $GaAlO_3$.

1073 K. This indicates that the catalysts tested here possess high thermal stability. However, the BET surface area summarized in Table 1 was found to decrease to almost 70% by calcination at 1073 K.

The dispersion of active species is sometimes improved by high-temperature calcination [22,23,25]. Fig. 5 shows XRD patterns of the metal oxide-doped Ga_2O_3–Al_2O_3 calcined at 1073 K along with non-doped Ga_2O_3–Al_2O_3. Although an increase in the intensity of XRD peaks assigned to $GaAlO_3$ was recognized for all the catalysts, the peaks ascribed to metal oxide additives were still not observed. In particular, the diffraction peaks assigned to CuO and Ag were diminished completely after the calcination at 1073 K. These results suggest that the dispersion of the additives was not lowered but was almost the same before and after the calcination at 1073 K. We think that this is one of the reasons for no activity depression by calcination at 1073 K.

3.5. Kinetic parameters of NO reduction by propene over In_2O_3–Ga_2O_3–Al_2O_3

As described above, In_2O_3–Ga_2O_3–Al_2O_3 showed the most remarkable activity enhancement by coexisting H_2O. In order to examine the influence of H_2O in the reaction mechanism, we performed kinetic studies for In_2O_3–Ga_2O_3–Al_2O_3 at 623 K. Here, In_2O_3–Ga_2O_3–Al_2O_3 calcined at 873 K was employed. Fig. 6 shows ln–ln plots of N_2 and CO_x ($CO + CO_2$) formation rates against the partial pressure of NO, C_3H_6 or O_2 (P_{NO}, $P_{C_3H_6}$ or P_{O_2}). Apparently, linear correlation was observed within experimental error. The N_2 formation rate in the presence of H_2O was higher than that in its absence at NO and C_3H_6 concentrations more than 520 and 480 ppm, respectively. Similar results were obtained for CO_x formation rate. Fig. 7 shows the Arrhenius plots for N_2 and CO_x formation rates in the presence and absence of H_2O.

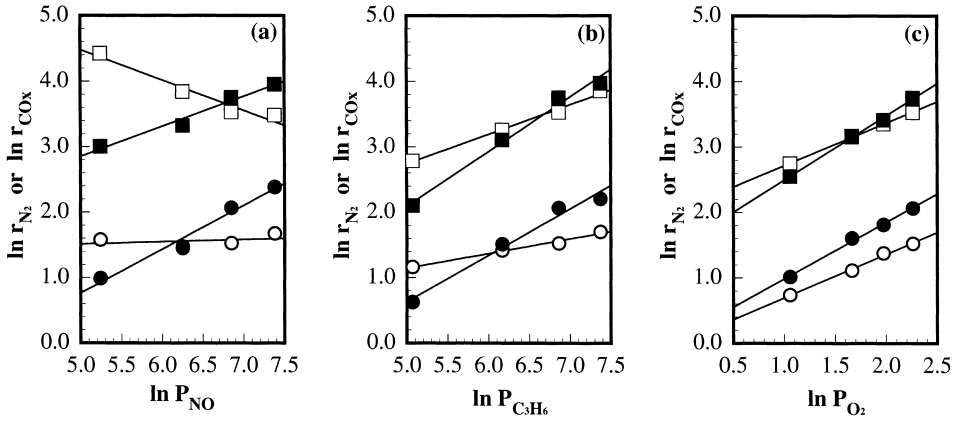

Fig. 6. Dependence of the formation rate of N_2 (○,●) and CO_x (□,■) in NO–C_3H_6–O_2 reaction system over In_2O_3–Ga_2O_3–Al_2O_3 on the partial pressure of (a) NO (200–1500 ppm), (b) C_3H_6 (200–1500 ppm) and (c) O_2 (3–10%). Solid symbols (●,■) indicate the results obtained in the presence of H_2O and open symbols (○,□) in its absence. Standard reaction conditions: NO = 900 ppm, C_3H_6 = 900 ppm, O_2 = 10%, H_2O = 0 or 9.1%, catalyst weight = 0.03–0.1 g, reaction temperature = 623 K, gas flow rate = 66 cm^3 min^{-1}.

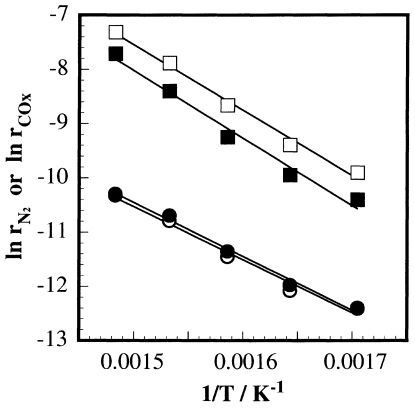

Fig. 7. Arrhenius plots for N_2 (○,●) and CO_x (□ ,■) formation rates in NO–C_3H_6–O_2 reaction system over In_2O_3–Ga_2O_3–Al_2O_3. Solid symbols (●,■) indicate the results obtained in the presence of H_2O and open symbols (○,□) in its absence. Reaction conditions: NO = 900 ppm, C_3H_6 = 900 ppm, O_2 = 10%, H_2O = 0 or 9.1%, catalyst weight = 0.03 g, gas flow rate = 66 cm^3 min^{-1}.

The kinetic parameters and the activation energies for N_2 and CO_x formation obtained are summarized in Table 2. The reaction orders with respect to NO, C_3H_6 and O_2 for N_2 and CO_x formation increased by the presence of H_2O. However, the activation energy was almost the same irrespective of coexisting H_2O. These results suggest that coexisting H_2O does not affect the total reaction steps but does affect several unit steps such as NO oxidation into NO_2 and reaction of NO_2 with propene to form N_2.

3.6. NO_x–TPD profiles

Fig. 8 shows the NO_x–TPD profiles of a mass number of 30 (NO), 32 (O_2) and 46 (NO_2) on Al_2O_3, Ga_2O_3–Al_2O_3 and In_2O_3–Ga_2O_3–Al_2O_3 after NO + O_2 adsorption. In this measurement, no desorption peak ascribed to N_2O was observed. Since NO_2 is known to decompose into NO inside the ionization chamber of the mass spectrometer, the desorption peak with a mass number of 30 is due to the sum of the parent mass of NO and the fragment mass of NO_2. Taking into account the ratio of the parent and fragment mass of NO_2, the amounts of NO_x (NO + NO_2) desorption integrated from the TPD measurements were calculated to be 129.4, 180.4 and 103.1 μmol g^{-1} for Al_2O_3, Ga_2O_3–Al_2O_3 and In_2O_3–Ga_2O_3–Al_2O_3, respectively. Apparently, the amount of NO_x desorbed from Ga_2O_3–Al_2O_3 was decreased by addition of In_2O_3, whereas its loading is relatively low (5 wt.%). We think the reason for the depression of NO_x adsorption ability of Ga_2O_3–Al_2O_3 by In_2O_3 as follows: (1) BET surface area of Ga_2O_3–Al_2O_3 was decreased ca. 10% by addition of In_2O_3. (2) Since In_2O_3–Ga_2O_3–Al_2O_3 was prepared by sol–gel method, In_2O_3 is presumed to be interacted strongly with Ga_2O_3 and Al_2O_3. We can consider that a large portion of NO_2 species seems to be adsorbed predominantly on Ga_2O_3–Al_2O_3 but not on In_2O_3.

Table 2
Kinetic parameters of the selective reduction of NO with propene over In_2O_3–Ga_2O_3–Al_2O_3[a]

Reaction system	Product	H_2O (%)	Reaction order[b] with respect to			Activation energy[c] (kJ mol^{-1})
			NO	C_3H_6	O_2	
NO–C_3H_6–O_2	N_2	0	0.0	0.2	0.7	81
		9.1	0.7	0.7	0.9	82
	CO_x	0	−0.4	0.5	0.7	98
		9.1	0.5	0.8	1.0	97

[a] Standard reaction conditions: NO = 900 ppm; C_3H_6 = 900 ppm; O_2 = 10%; H_2O = 0 or 9.1%; reaction temperature = 623 K; gas flow rate = 66 cm^3 min^{-1}.
[b] Reaction conditions: NO = 200–1500 ppm; C_3H_6 = 200–1500 ppm; O_2 = 3–10%; catalyst weight = 0.03–0.1 g.
[c] Activation energies were calculated by varying the temperatures from 623 to 723 K.

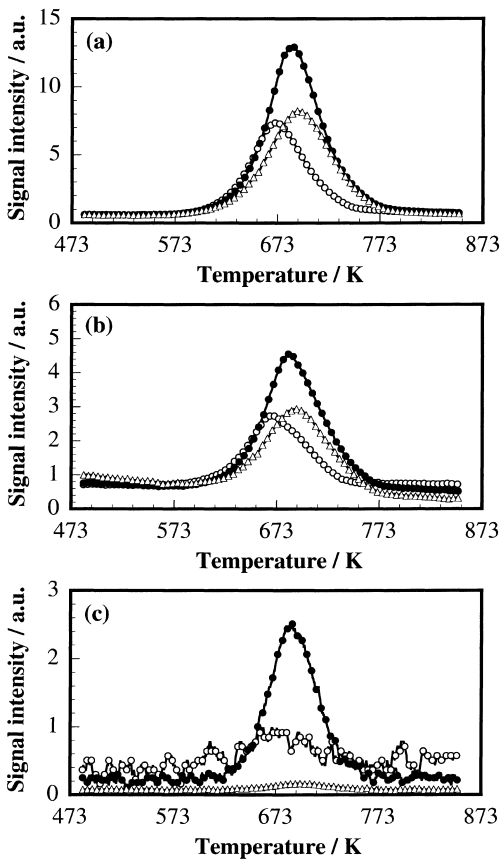

Fig. 8. TPD profiles of (a) NO (mass number: 30), (b) O_2 (32) and (c) NO_2 (46) on Al_2O_3, Ga_2O_3–Al_2O_3 and In_2O_3–Ga_2O_3–Al_2O_3. The samples were pretreated in flowing 10% O_2/He at 873 K for 1 h, followed by NO adsorption in flowing 1000 ppm NO/10% O_2/He at room temperature for 2 h. TPD measurements were carried out up to 873 K with a heating rate of 5 K min^{-1} in flowing He (60 cm^3 min^{-1}). (△) Al_2O_3, (●) Ga_2O_3–Al_2O_3, (○) In_2O_3–Ga_2O_3–Al_2O_3.

3.7. Influence of H_2O on reaction pathway

A lot of reaction mechanisms have been proposed so far concerning the selective NO reduction by hydrocarbons. Concerning alumina-based catalysts, a mechanism that NO is first oxidized to NO_2 and subsequently the resulting NO_2 reacts with hydrocarbon-derived species to form N_2 and CO_x is supported by many researchers [22,23,26,27]. In the present work, we think that NO reduction by propene over In_2O_3–Ga_2O_3–Al_2O_3 proceeds through a similar reaction pathway. NO_x–TPD profiles given in Fig. 8 shows that a lot of NO_x species, probably NO_3^- adspecies, are still adsorbed on In_2O_3–Ga_2O_3–Al_2O_3 in the temperature range between 573 and 773 K, where NO reduction takes place effectively. Propene is known to be easily converted into allyl species, which is one of the candidates of C_3H_6-derived species, by H-abstraction [28,29]. Therefore, we propose a reaction pathway that NO_2, probably adsorbed NO_3^- species, reacts with C_3H_6-derived species like allyl species to produce N_2 and CO_x.

As can be seen in Table 2, the activation energy was not changed by H_2O, suggesting that coexisting H_2O does not change the total reaction steps but change the rate-determining step. If the reaction of NO_2 with C_3H_6-derived species is sufficiently fast, the reaction order with respect to C_3H_6 for N_2 formation and that to NO for CO_x formation should be nearly unity. When the reaction was carried out in the absence of H_2O, the former value was 0.2 and the latter one was –0.4. This suggests that the reaction of NO_2 with C_3H_6-derived species is sufficiently slow, probably the rate-determining step, meaning that C_3H_6-derived species are gradually accumulated on

the catalyst surface. This is consistent with our previous report [30] that carbonaceous materials deposited on In_2O_3–Ga_2O_3–Al_2O_3 during NO reduction by propene in the absence of H_2O inhibit the reaction.

With respect to the reaction in the presence of H_2O, on the other hand, the reaction orders for all the reactants were increased considerably and were brought close to nearly unity. This suggests that adsorption of NO_x and C_3H_6 leading to NO_3^- and C_3H_6-derived species, respectively, takes place competitively on the catalyst surface. We also reported that coexisting H_2O efficiently acts to remove the surface carbonaceous materials [30]. Therefore, we suppose that the reaction of NO_2 with C_3H_6-derived species as precursors of carbonaceous materials is fast and that the formation of C_3H_6-derived species is slow, probably the rate-determining step. We observed that propene conversion on In_2O_3–Ga_2O_3–Al_2O_3 in the reaction system of $NO + C_3H_6 + O_2$ was intensified considerably by the presence of H_2O (Fig. 3). The formation rate of C_3H_6-derived species in the presence of H_2O might be sufficiently fast compared with the reaction rate of NO_2 with C_3H_6 or C_3H_6-derived species in the absence of H_2O. This is probably the reason for the promotional effect of H_2O.

3.8. Influence of coexisting SO_2 on the activity of metal oxide-doped Ga_2O_3–Al_2O_3

The catalytic activity of metal oxide-doped Ga_2O_3–Al_2O_3 for NO reduction by propene in the presence of H_2O and SO_2 was next examined. Here, we chose Ga_2O_3–Al_2O_3, In_2O_3-, SnO_2- and CoO–Ga_2O_3–Al_2O_3 calcined at 873 K, which showed excellent activity in the presence of H_2O as indicated in Fig. 3. The results are given in Fig. 9. As can be seen by comparing Figs. 3 and 9, the NO reduction activity of all the catalysts was decreased by the presence of SO_2. In particular, a considerable retarding effect of SO_2 was observed for In_2O_3- and CoO–Ga_2O_3–Al_2O_3 on which the maximum NO conversion was dropped from 93% at 673 K to 68% at 723 K and from 84% at 723 K to 49% at 773 K, respectively. Of the catalysts tested here, a maximum NO conversion of 77% was attained on Ga_2O_3–Al_2O_3 at 773 K. It is noted that SnO_2–Ga_2O_3–Al_2O_3 showed the most excellent activity at lower temperatures than 723 K.

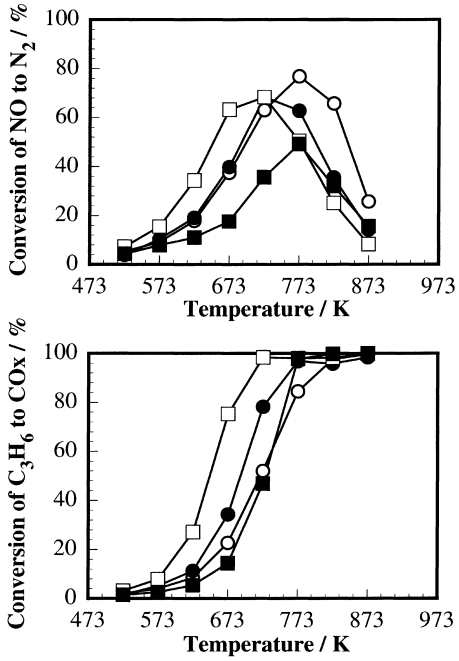

Fig. 9. Effect of SO_2 on the catalytic activity of metal oxide-doped Ga_2O_3–Al_2O_3 calcined at 873 K for NO reduction by propene in the presence of H_2O. Conditions: NO = 900 ppm, C_3H_6 = 900 ppm, O_2 = 10%, H_2O = 9.1%, SO_2 = 90 ppm, catalyst weight = 0.2 g, W/F = 0.18 gscm^{-3}. (○) Ga_2O_3–Al_2O_3, (●) In_2O_3–Ga_2O_3–Al_2O_3, (□) SnO_2–Ga_2O_3–Al_2O_3, (■) CoO–Ga_2O_3–Al_2O_3.

Table 3
Summary of BET surface area of the fresh and spent catalysts

Catalyst	BET surface area ($m^2\,g^{-1}$)	
	Fresh catalyst	Spent catalyst
Ga_2O_3–Al_2O_3	200	163
In_2O_3–Ga_2O_3–Al_2O_3	185	162
SnO_2–Ga_2O_3–Al_2O_3	200	175
CoO–Ga_2O_3–Al_2O_3	175	162

In order to examine the effect of SO_2 on the physical properties of the catalysts, we performed characterization of the catalysts before (fresh) and after (spent) the reaction in the presence of SO_2. BET surface areas of the fresh and the spent catalysts are summarized in Table 3. Although decreases of BET surface area due to SO_2 were recognized for all the catalysts, relatively high surface area more than 160 $m^2\,g^{-1}$ was still maintained. It was also found from XRD measurements that the crystallite structure did not change at all. This fact indicates that SO_2 was not incorporated

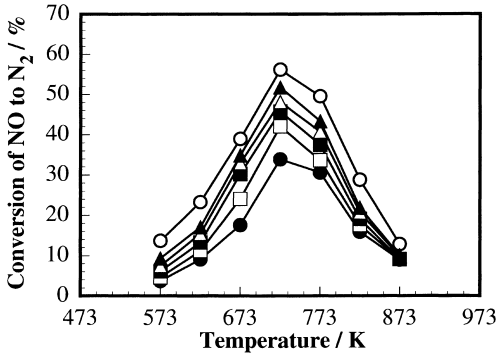

Fig. 10. Effect of SO_2 concentration on the catalytic activity of SnO_2–Ga_2O_3–Al_2O_3 for NO reduction by propene in the presence of H_2O. Conditions: NO = 900 ppm, C_3H_6 = 900 ppm, O_2 = 10%, H_2O = 9.1%, SO_2 = 0–270 ppm, catalyst weight = 0.05 g, W/F = 0.045 gscm^{-3}. (○) SO_2 = 0 ppm (fresh), (●) SO_2 = 270 ppm, (□) SO_2 = 90 ppm, (■) SO_2 = 45 ppm, (△) SO_2 = 23 ppm, (▲) SO_2 = 0 ppm (after the reaction in the presence of SO_2).

into the bulk. Tabata et al. [31] observed sulfate species (SO_4^{2-}) formed on Al_2O_3 by measuring FT–IR spectra of Al_2O_3 and Sn/Al_2O_3 used for NO reduction in the presence of H_2O and SO_2. In the present work, a similar phenomenon, namely, the formation of sulfate species on the catalytically active sites in the vicinity of the catalyst surface, should take place during NO reduction in the presence of SO_2. We think that the formation of surface sulfate species is one of the reasons for the activity depression by SO_2.

3.9. Effect of SO_2 concentration on the activity of SnO_2–Ga_2O_3–Al_2O_3

We examined the effect of SO_2 concentration on the activity of SnO_2–Ga_2O_3–Al_2O_3 for NO reduction by propene in the presence of H_2O. The W/F was set at 0.45 gscm^{-3} (SV = 50 000 h^{-1}) and the concentration of SO_2 was changed from 270 to 0 ppm. During the series of experiments changing SO_2 concentration, the catalyst sample was not replaced to new one. As shown in Fig. 10, the catalytic activity decreased monotonously with increasing SO_2 concentration. Removing SO_2 from the reaction gas mixture restored ca. 90% of the initial activity. This means that the deactivation by SO_2 is almost reversible. Since the decomposition of tin sulfate ($SnSO_4$) is known to initiate at 633 K, adsorption and desorption of SO_2 would be in equilibrium during the reaction.

Fig. 11(a) shows the change in NO conversion on SnO_2–Ga_2O_3–Al_2O_3 against the logarithm of SO_2 concentration at several reaction temperatures. A good linear relationship was observed at all the reaction temperatures. The slope, abbreviated as α, which indicates the inhibiting effect of SO_2, shows that the extent of deactivation by SO_2 becomes small at elevated temperatures. In Fig. 11(b), the reaction temperature was plotted against the negative value of α. The reaction temperature at which the value of α becomes zero was found to be ca. 830 K. This means that no deactivation takes place at this temperature. We think that

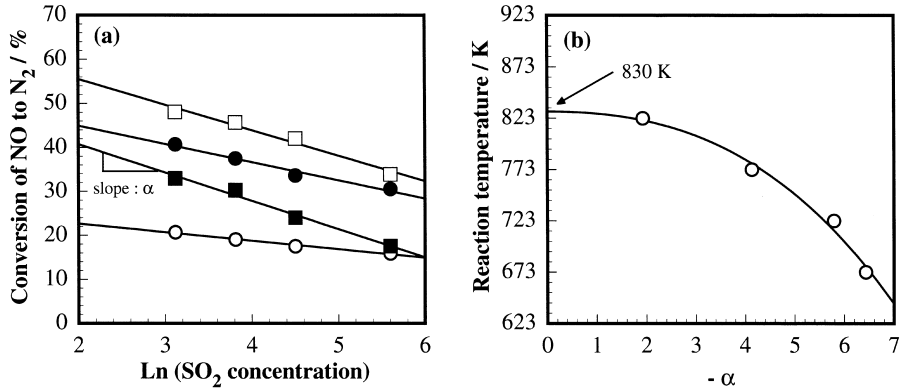

Fig. 11. (a) Change in NO conversion on SnO_2–Ga_2O_3–Al_2O_3 with SO_2 concentration. The reaction conditions are the same as for Fig. 10. (○) 873 K, (●) 823 K, (□) 773 K, (■) 723 K. (b) Relationship between negative value of the slope 'α' calculated in (a) and the reaction temperature.

the catalyst deactivated by SO_2 might be regenerated by treating at elevated temperatures above 830 K.

4. Conclusions

The catalytic performance of several metal oxide-doped Ga_2O_3–Al_2O_3 for the selective reduction of NO with propene was investigated. Although the addition of CoO, CuO and Ag into Ga_2O_3–Al_2O_3 enhanced the activity for NO reduction in the absence of H_2O, their activities were depressed considerably by the presence of H_2O. On the other hand, a considerable promotional effect of H_2O was observed for In_2O_3- and SnO_2–Ga_2O_3–Al_2O_3, especially in the lower temperature region below 623 K. Accordingly, these two catalysts showed the highest activity in the presence of H_2O. Calcination at 1073 K did not change the activity, suggesting that the catalysts tested here possess relatively high thermal stability. The kinetic studies on In_2O_3–Ga_2O_3–Al_2O_3 for NO reduction by propene in the presence and absence of H_2O revealed that coexisting H_2O affects strongly the reaction steps in which NO_x species participate. A reaction pathway was proposed that NO_2 formed on Ga_2O_3–Al_2O_3 reacts with C_3H_6-derived species, probably allyl species produced by H-abstraction, to produce N_2 and CO_x. As for the reaction in the absence of H_2O, the reaction of NO_2 with C_3H_6-derived species is the rate-determining step, while as for that in its presence, the formation of C_3H_6-derived species is slow. The addition of SO_2 into the reaction gas caused a decrease of NO conversion on all the catalysts due to formation of sulfate species (SO_4^{2-}). However, SnO_2–Ga_2O_3–Al_2O_3 showed relatively high resistivity against SO_2 and the deactivation was found to be almost reversible.

References

[1] M. Iwamoto, Catal.Today 29 (1996) 29.
[2] M.D. Amiridis, T. Zhang, R.J. Farrauto, Appl. Catal. B 10 (1996) 203.
[3] M. Iwamoto, H. Yahiro, S. Shundo, Y. Yu-u, N. Mizuno, Appl. Catal. 69 (1991) L15.
[4] C. Yokoyama, M. Misono, Catal. Today 22 (1994) 59.
[5] T. Tabata, M. Kokitsu, H. Ohtsuka, O. Okada, L.M.F. Sabatino, G. Bellussi, Catal. Today 27 (1996) 91.
[6] E. Kikuchi, K. Yogo, Catal. Today 22 (1996) 73.
[7] R. Burch, P.J. Millingtona, A.P. Walker, Appl. Catal. B 4 (1994) 65.
[8] G. Zhang, T. Yamaguchi, H. Kawakami, T. Suzuki, Appl. Catal. B 1 (1992) L15.
[9] A. Obuchi, A. Ohi, M. Nakamura, A. Ogata, K. Mizuno, H. Ohuchi, Appl. Catal. B 2 (1993) 71.
[10] Y. Kintaichi, H. Hamada, M. Tabata, M. Sasaki, T. Ito, Catal. Lett. 6 (1990) 239.
[11] Y. Torikai, H. Yahiro, N. Mizuno, M. Iwamoto, Catal. Lett. 9 (1991) 91.
[12] T. Miyadera, K. Yoshida, Chem. Lett. (1993) 1483.
[13] H. Hamada, Catal. Today 22 (1994) 21.
[14] R.A. Grinstedt, H.-W. Jen, C.N. Montreuil, M.J. Rokosz, M. Shelef, Zeolites 13 (1993) 602.
[15] M. Iwamoto, H. Yahiro, H.K. Shin, M. Watanabe, J. Guo, M. Konno, T. Chikahisa, T. Murayama, Appl. Catal. B 5 (1994) L1.
[16] R. Keiski, H. Raisanen, M. Harkonen, T. Maunula, P. Niemisto, Catal. Today 26 (1996) 85.
[17] M. Haneda, Y. Kintaichi, H. Shimada, H. Hamada, Chem. Lett. (1998) 181.
[18] K. Shimizu, H. Maeshima, A. Satsuma, T. Hattori, Appl. Catal. B 18 (1998) 163.
[19] N. Aoyama, K. Yoshida, A. Abe, T. Miyadera, Catal. Lett. 43 (1997) 249.
[20] K.A. Bethke, H.H. Kung, J. Catal. 172 (1997) 93.
[21] M. Haneda, Y. Kintaichi, M. Inaba, H. Hamada, Bull. Chem. Soc. Jpn. 70 (1997) 499.
[22] H. Hamada, Y. Kintaichi, M. Inaba, M. Tabata, T. Yoshinari, H. Tsuchida, Catal. Today 29 (1996) 53.
[23] N. Okazaki, Y. Katoh, Y. Shiina, A. Tada, M. Iwamoto, Chem. Lett. (1997) 889.
[24] T. Maunula, Y. Kintaichi, M. Inaba, M. Haneda, K. Sato, H. Hamada, Appl. Catal. B 15 (1998) 291.
[25] J.Y. Yan, M.C. Kung, W.M.H. Sachtler, H.H. Kung, J. Catal. 172 (1997) 178.
[26] H. Hamada, Y. Kintaichi, M. Sasaki, T. Ito, M. Tabata, Appl. Catal. 70 (1991) L15.
[27] M. Sasaki, H. Hamada, Y. Kintaichi, T. Ito, Catal. Lett. 15 (1992) 297.
[28] F. Radtke, R.A. Koeppel, E.G. Minardi, A. Baiker, J. Catal. 167 (1997) 127.
[29] N.W. Hayes, R.W. Joyner, E.S. Shpiro, Appl. Catal. B 8 (1996) 343.
[30] M. Haneda, Y. Kintaichi, H. Hamada, Catal. Lett. 55 (1998) 47.
[31] M. Tabata, T. Yoshinari, K. Miyamot, H. Yamazaki, H. Hamada, J. Jpn. Inst. Energy 75 (1996) 424.